Scalable Near-field Fed Far-field UHF RFID Reader Antenna for Retail Checkout Counters

Prabakar Parthiban, Boon-Chong Seet and Xue Jun li
Department of Electrical and Electronic Engineering
Auckland University of Technology
Auckland 1010, New Zealand

{prabakar. Parthiban, boon-chong.seet and xuejun.li}@aut.ac.nz

***Abstract*— This paper presents a scalable ultra-high-frequency (UHF) radio frequency identification (RFID) reader antenna for retail checkout counters. The antenna's simultaneous near-field and far-field operation enable effortless and reliable asset identification. Two meandered microstrip lines that are 90° out-of-phase form the near-field antenna rim around a far-field patch antenna. The patch antenna is fed by those meandered lines along the vertices on its orthogonal points, resulting in circular polarization. The near-field radiation is evenly distributed with no surface dead zones, and the far-field radiation pattern is symmetrical with a 90° half-power beam-width in both azimuth and elevation planes. The antenna operates in the North American UHF RFID band (902-928 MHz) with a 50 MHz impedance bandwidth. The antenna's gain and axial ratio at the band's center frequency of 915 MHz is 3.3 dBi, and 1.4 dB, respectively. This antenna is low-profile, low-cost and recyclable as it is constructed from polyolefin substrate and copper foils.**

Keywords—RAIN RFID; meander-line; passive antenna; low-profile; patch antenna; near-field; far-field; circular polarization; point-of-sale.

I. INTRODUCTION

UHF RFID is a part of Automatic Identification and Data Capture (AIDC) system which collects information from an object or an individual without needing a manual data entry. Industry associations such as the Advancing Identification Matters (AIM) and RAdio frequency IdentificatioN (RAIN) promote the global adoption for UHF RFID that utilizes the GS1 UHF Gen2 protocol as per ISO/IEC 18000-63 standard. The industry 4.0 focus on automation of manufacturing and data management demands the need for UHF RFID along with other Internet-of-Things (IoT) devices. A typical UHF RFID system consists of a reader and antenna to transmit and receive RF signals, a tag with a unique identifier, and a computer with appropriate software to post-process the data.

This paper proposes a new UHF RFID reader antenna design with simultaneous near-field (NF) and far-field (FF) operations for retail checkout counters, otherwise known as the point-of-sale (POS). UHF RFID is attractive for retail industries due to its simplicity, compatibility, and cost-effectiveness in installation and maintenance [1]. Asset tracking is often challenging at the POS as the assets are heterogeneous, made of materials varying from paper, plastics, linen to metals and liquids. Assets will be at proximity to the reader antenna at POS while billing and checking out. Traditional FF antennas are very sensitive to these proximity assets. High dielectric assets and metal assets detune the FF antenna whereas liquid assets limit the antenna's read range [2]. NF antennas can solve this problem as the magnetic fields are less affected by liquid and metal assets, but the read-range is significantly less compared to the FF antenna. Antennas that can operate in both NF and FF simultaneously is an essential requirement for retail POS application. Other vital requirements for retail checkout counter reader antennas include:

- Customizable size in the 2-D plane to suit different checkout counters such that the scanning area is occupied by the NF and FF energy with no surface dead zones
- Low gain and uni-directional FF radiation to avoid reading unwanted proximity items
- Symmetrical wide-beam FF radiation to provide adequate coverage over the checkout counters
- Low-profile and embeddable under the counter or checkout conveyor belt
- Mechanically sturdy to accustom heavy assets laid on them
- Low-cost construction for ease of adoption by retail industry

This paper presents a perimetric meandered line fed patch antenna, in which the meandered line creates a square rim of NF radiation and the center patch produces directional FF radiation. The NF perimetric rim has a uniform energy distribution on its surface with no dead zones. The circularly polarized patch creates a symmetrical radiation pattern that enables accurate tag detection regardless of the asset's orientation. The perimetric NF antenna's size in 2D-plane is scalable with increase in counter size and customizable for various retail checkout counters.

978-1-7281-1210-7/19/$31.00 ©2019 IEEE

Scaling the patch antenna is not required as its symmetrical wide-beam is sufficient to cover large- and small-sized counters. The antenna is low-profile and constructed from non-conventional polyolefin substrate with inherent properties such as UV/impact/chemical resistance, low coefficient of friction, light-weight and high durability [3]. The antenna is designed for the North American UHF RFID frequencies (902-928 MHz). With an impedance bandwidth of 50 MHz which is larger than the required operating bandwidth of 26 MHz, the excess bandwidth of our antenna can be useful to accommodate any detuning (frequency shift) caused by the proximity assets. Power reflections induced by nearby metallic assets are drained through a resistor on the isolation port of a quadrature hybrid coupler (to achieve circular polarization in the patch), thus preventing permanent damage to the RFID readers [4].

II. Related Works

Several UHF RFID reader antenna designs that can operate either in NF [5-7] or FF [8-10] have been recently proposed. The NF designs are typically based on segmented loops, meandered line, travelling-wave and oppositely directed current (ODC) antennas [2], while the FF designs often used microstrip patch, stacked patch, quasi-Yagi, monopoles, dipoles, PIFA, helical, slot and loop antennas [X]. Existing antenna designs that can operate in both NF and FF are not suitable for retail checkout counter/POS applications.

The multiport reader antenna design in [11] is a dipole-based design where four dipoles are arranged in a square geometry and fed at a different location using three ports. The antenna behaves as an NF antenna when fed at port-A and resonates with two different orthogonal linear polarization when excited through port-B and port-C, respectively. The main disadvantage with this design is that the users will have to either use three different RFID readers (if they are 1-port readers) or a 3-port reader in order to use this antenna, which increases the cost and complexity of the system. The antenna's bidirectional radiation may read unwanted stray tags in a POS scenario, and its half-power beam-width (HPBW) is not measured. On the other hand, our proposed antenna in this paper can operate in both NF and FF simultaneously when excited using a single port. It is circularly polarized, has a directional radiation pattern, and customizable NF readable region.

A fragment type structure is designed in [12] for simultaneous NF and FF operation, producing bidirectional radiation with 60°, and 90° HPBW, respectively, which can introduce stray tag reads. The antenna's impedance matching and frequency of operation are dependent on the structure's length and width and internal connections. Fabrication cost and complexity are higher in this antenna as there are a lot of variables that need great precision and attention. Although the NF and FF operation can be performed simultaneously, the FF radiation is only linearly polarized, which cannot detect tags in different orientations. In contrast, our proposed antenna can simultaneously operate in NF and circularly polarized FF. Furthermore, its directional radiation can create a predictable read zone that will not induce stray tag detection. Comparatively, it is a less-complex design that can scale without any significant modification of the antenna's critical parameters such as its impedance and frequency of operation.

A switchable NF/FF antenna is presented in [13], which has a PIN diode that operates the antenna in those two modes when biased with different voltages. Four dipole antennas arranged in a square geometry (as in [11]) are driven with equal phase for NF operation and with incremental phase delays of 0°, 90°, 180° and 270° for FF operation. The FF antenna is circularly polarized with an axial ratio of 1.5 dB. The antenna's 50° HPBW is narrow for POS applications and may miss assets that travel through the checkout counter conveyors. On the contrary, our proposed antenna is passive and can operate in both NF and FF simultaneously without the need of switching. Losses introduced by PIN diodes do not exist in our proposed design. Moreover, there is no need for DC biasing in our design, which eases the installation.

The authors in [14] presented a linearly polarized coupled loop antenna design that operates in NF and FF simultaneously with a bidirectional radiation whose HPBW is 90°, and 75°, respectively. As the loop is a function of the wavelength, scaling this antenna design is impossible without trading-off its performance. The antenna's overall thickness with a reflector is 80 mm. Unlike the above antenna, our proposed antenna is low-profile, mechanically sturdy, UV/chemical/impact resistant, and low moisture absorbent. In addition, it has a uni-directional and symmetrical radiation pattern with 90° HPBW in both planes.

The compact multiservice reader antenna designed for NF and FF application in [15] is a circularly polarized antenna with 3 dB axial ratio. The antenna is based on a rectangular slot design fed by L-shaped feed. The asymmetric slot perturbation yields the circularly polarized fields. The antenna's radiation is uni-directional and symmetrically spread in both planes with an HPBW of 80°. Unlike our proposed antenna, this antenna is hardly scalable as the dimensions of its slots cannot be altered to suit checkout counters with different sizes. Moreover, its 3 dB axial ratio can make tag detection harder when assets are oriented in different planes. On the other hand, our proposed antenna's NF region is easily scalable by altering the meandered line to suit the dimensional requirements. In addition, its axial ratio is twice as large as the existing design. Reflections caused by nearby metallic assets are drained through a termination resistor in the proposed design while they are fed directly back to the RFID reader in [15].

The meandered line antenna presented in [16] is a near-field antenna that can also detect far-zone items. These antennas cannot detect tags whose orientations are orthogonal to the prescribed orientation, unlike our proposed design. The meandered lines are unterminated (by a load) and their width, spacing and turns have to be fixed, otherwise the antenna's resonance will be affected, highlighting its inability to scale to different sizes. On the other

hand, our patch antenna terminates the meandered lines, and can scale in both axes of the 2-D plane.

III. Antenna Design and Fabrication

Our antenna design features a radiating patch that is driven along the vertices by two meandered microstrip lines. To achieve circular polarization, the patch must be driven 90° out-of-phase with an equal magnitude on its orthogonal points which can be either along the vertices or along the perpendicular bisectors intersecting the sides, where TM_{01} and TM_{10} modes exist. A 6 mm high-density polyethylene (HDPE, a type of polyolefin) sheet is used as the substrate whose dielectric constant (ε_r) and loss tangent is 2.256 and 0.0002, respectively [3]. The patch is inset-fed at a location 21 mm along the diagonals, which is 16.8 mm away from the sides (See Fig.1). The patch's impedance at this location is found to be 113 Ω.

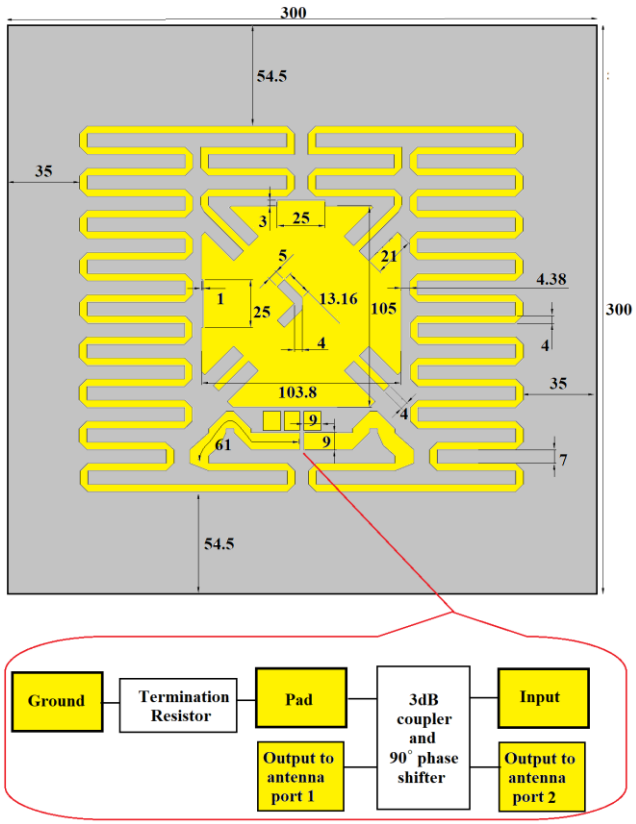

Fig. 1. Proposed antenna design with input components

The microstrip line consists of a quarter-wave transformer that transforms the 50 Ω input impedance into 113 Ω patch impedance. The length and width of the quarter-wave transformer are 61 mm and 9 mm, respectively. The 113 Ω microstrip line is meandered around the patch in all four directions to inset feed the patch along its diagonals. The meandered microstrip line creates a strong magnetic field on the antenna surface contributing to the NF radiation while the patch produces the FF radiation. The magnetic field is evenly distributed on the surface of meandered lines with no dead zones. The NF area can be extended along the antenna's surface in its X and Y axes just by lengthening the meanders in the microstrip line, thereby enhancing the scalability.

A low-loss, thin-film, 3dB hybrid coupler that has four ports: input port, isolation port and two output ports with nominal 50 Ω impedances, is used. The small-sized coupler helps to eliminate dead zones around it. The input power is divided equally through two output ports with 90° phase difference. Although the coupler offers high isolation, it is recommended to terminate the isolation port with a 50 Ω thin-film resistor to maintain balanced coupling. The coupler's output ports are connected to the patch via the meandered lines to generate circularly polarized waves. The patch is tuned using tuning stubs and 'V' slots to withstand the electromagnetic coupling experienced between the meandered lines and the patch. The patch's size is calculated to be 105 mm long and 103.8 mm wide, which are dependent on the substrate's ε_r and thickness. For more compact patch size, thicker substrate with higher ε_r may be used. Although the width of the patch is physically shorter, the 'V' slot makes the patch electrically wider.

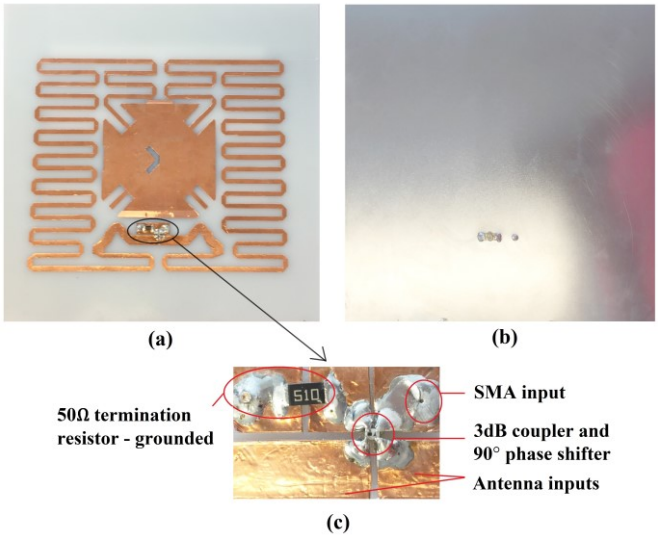

Fig. 2. Fabricated antenna (a) radiator and feed network (b) ground plane with SMA connector (c) components at the input

The D4 symmetry of the patch is maintained by introducing a dummy replica of the inset-feed on its other half [17]. Fig. 1 shows the construction of the meandered line fed patch antenna. The coupler's input port is connected to a rear-mount SMA connector. Both the patch and meandered lines are fabricated using a 0.1 mm copper foil. The ground plane is constructed using a 0.2 mm tinned steel sheet (See Fig.2).

The copper foil and the tinned sheets are adhered to the HDPE using non-conductive acrylic adhesive that has 125 N/100 mm adhesion to metal and 86 N/100 mm adhesion to plastic. The coupler, SMA connector, 50 Ω resistor and its grounding pin used are soldered directly onto the copper foil. Fig. 2 shows the coupler and 50 Ω termination resistor in the fabricated antenna.

IV. Measurement Analysis

The fabricated antenna's performance was measured using a TR/1300 VNA in an anechoic chamber. The linear gain of the antenna is measured for both vertical and horizontal polarization by the comparative method using a calibrated reference antenna. The antenna's return loss and gain values in the FCC operating band are shown in Fig. 3 (highlighted), and in Table I for low, mid and high frequencies of the FCC band. The antenna has a 50 MHz and 42 MHz return loss bandwidth at -10 dB, and -15 dB cut-off, respectively. The antenna's peak gain at 915 MHz in vertical polarization is 3.3 dBi with 1.4 dB axial-ratio. The antenna's best- and worst-case axial-ratio is 0.8 dB at 902 MHz and 2.2 dB at 928 MHz, respectively.

TABLE I. Measurements at FCC frequencies

Parameter	902 MHz	915 MHz	928 MHz
Return loss (dB)	-17.2	-16.4	-19.6
Vertical polarized gain (dBi)	2.4	3.3	0.5
Horizontal polarized gain (dBi)	1.6	1.9	2.7

The FF radiation pattern is given in Fig. 4, which shows a symmetrical radiation pattern with 90° HPBW in both elevation and azimuth planes. The fabricated antenna is tag tested to benchmark the RFID metrics. An Impinj speedway R420 RFID reader [18] (FCC band) is used for testing purposes. Smartrac's 'Miniweb' and 'Bling' tags are used for testing. The former is specially designed for general asset tracking and supply-chain application [19] while the latter is for jewelry, cosmetics and other close-coupled applications [20]. The antenna's NF and FF radiation are tested by presenting the tag directly on top of, and above the antenna, respectively. The 300 mm × 300 mm antenna is divided into 36 cells, each being 50 mm × 50 mm. Fig. 5 shows the test setup with grids marked on the antenna's surface. One tag per cell is placed and tested for its return signal strength (RSSI) for vertical and horizontal tag-orientation. The bling tag and the Miniweb tag spans 25 × 15 mm and 42 × 16mm, respectively.

The Impinj's item sense software is used to retrieve RSSI information by setting the reader to two different power levels: 10 dBm (min) and 31.5 dBm (max). It is observed that the NF distribution is concentrated on the antenna's surface for Bling and the surface detection range is extended by 50 mm laterally in both axes for Miniweb tag. Fig. 6 and Fig. 7 shows the contour plot of the Bling and Miniweb tag's RSSI, respectively, over the antenna's surface for two power settings (min and max) and orthogonal tag orientations (vertical and horizontal). Fig. 8 shows the maximum read distance plot for both tags at 10 dBm power. A summary of the performance differences between the proposed and existing antenna designs is provided in the Table II.

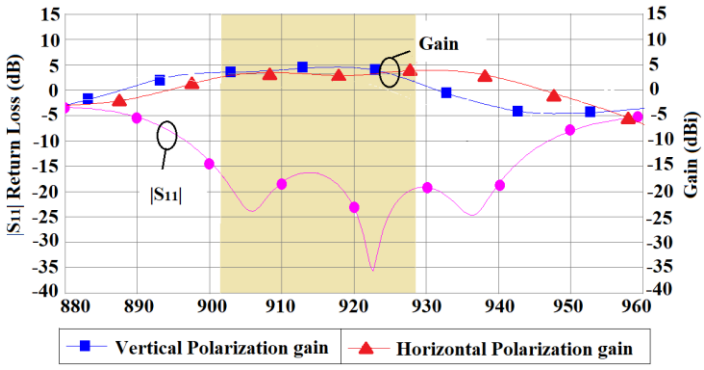

Fig. 3. Return loss and gain measurements

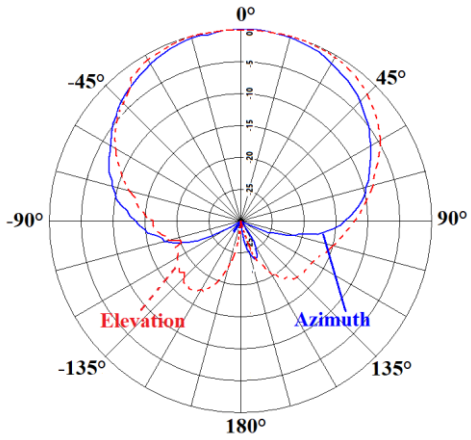

Fig. 4. Far-field radiation pattern

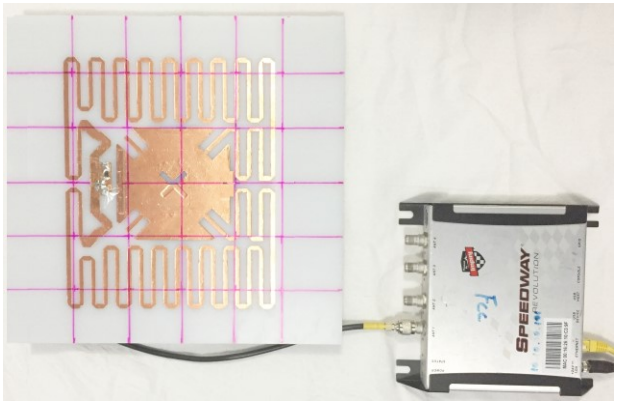

Fig. 5. Tag testing setup

TABLE II. PROPOSED ANTENNA DESIGN VS EXISTING DESIGNS SUMMARY OF PERFORMANCE DIFFERENCES

Ref.	FF Polarization	Gain (f_c)	Axial ratio (f_c)	FF HPBW (f_c)	FF radiation	DC Bias Required?	Ports required	Simultaneous NF and FF operation?	NF zone Scalability	Reflection handling ability
[11]	Linear	-3.2 dBi	Infinity	Not measured	Bi-directional	No	Three	No	No	No
[12]	Linear	5 and 6 dBi	Infinity	60° and 90°	Bi-directional	No	One	Yes	No	No
[13]	Circular	7 dBiC	1.5 dB	50°	Directional	Yes	One	No	No	Yes (Wilkinson power dividers)
[14]	Linear	6.8 dBi	Infinity	90° and 75°	Bi-directional	No	One	Yes	No	No
[15]	Circular	5.5 dBiC	3 dB	80°	Directional	No	One	Yes	No	No
[16]	Linear	-5 dBi	Infinity	Not measured	Directional	No	One	Yes	No	No
This paper	Circular	3.3 dBi (5.3 dBiC)	1.4 dB	90° in both planes	Directional	No	One	Yes	Yes	Yes (Quadrature hybrid coupler)

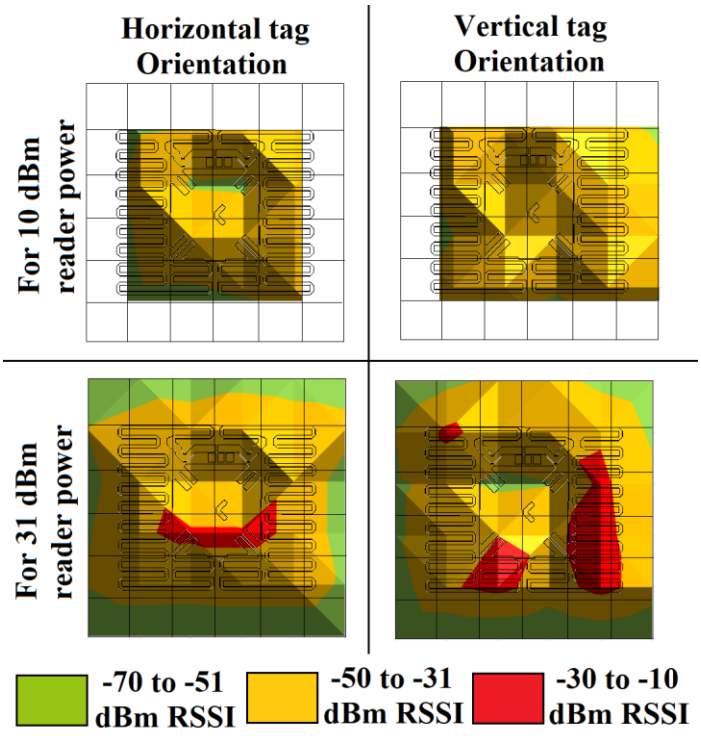

Fig. 6. Bling tag's RSSI measurements

The change in color per unit cell implies that the transmitted signal strength in those zones with respect to the tag's ability to receive the signals. It is clear that the Miniweb tag has a greater ability than the Bling tag to receive the signal in the unit cells.

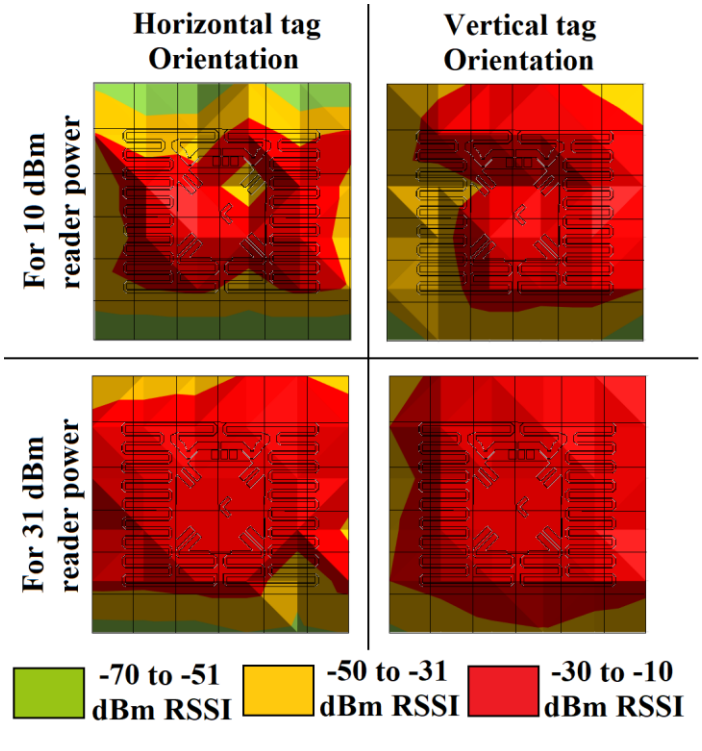

Fig. 7. Miniweb tag's RSSI measurements

On the other hand, the Bling tag was not detected in some cells at 10 dBm reader power as shown by the uncolored cells in Fig. 6 (top row). Fig. 8 shows the maximum read distance plot for both tags at 10 dBm power.

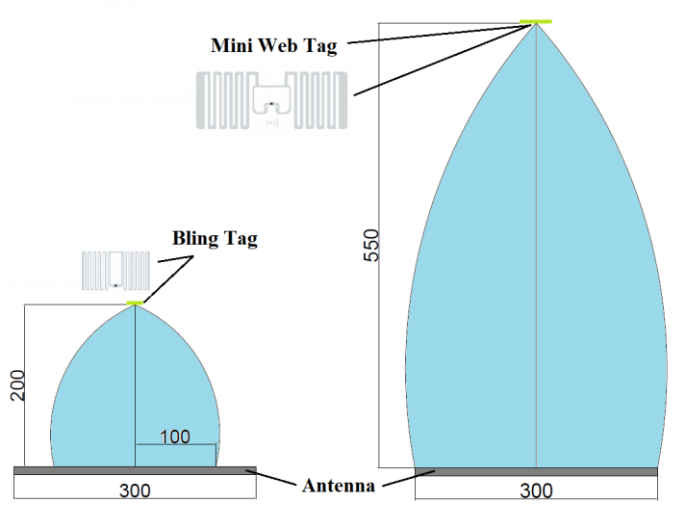

Fig. 8. Read distance measurements (units in mm) for Bling and Mini-web tags

V. Conclusion

A new scalable UHF RFID near-field fed far-field reader antenna design is proposed to meet the requirements for POS reader antenna at retail checkout counters. The design features a meandered line fed patch antenna that yields a 3.3 dBi (5.3 dBiC) peak gain with a 90° half-power beam-width in both planes. The antenna's axial ratio is 1.4 dB at f_c. The antenna operates between 902 and 928 MHz (North American RFID frequencies) and has uniform surface energy distribution with no dead zones. Furthermore, it is low-cost, planar and mechanically sturdy with excellent UV/chemical/impact resistant properties and low friction coefficient. A similar reader antenna is currently being designed to cover the European RFID frequencies from 865 to 868 MHz.

Acknowledgment

The first author would like to thank Times-7 Research Ltd for their constant support and encouragement towards his Ph.D. research at the Auckland University of Technology, New Zealand.

References

[1] G. Xiao *et al*., "Printed UHF RFID Reader Antennas for Potential Retail Applications," IEEE Journal of Radio Frequency Identification, vol. 2, no. 1, pp. 31-37, March 2018.

[2] A. Michel, P. Nepa, X. Qing and Z. N. Chen, "Considering High-Performance Near-Field Reader Antennas: Comparisons of Proposed Antenna Layouts for Ultrahigh-Frequency Near-Field Radio-Frequency Identification," IEEE Antennas and Propagation Magazine, vol. 60, no. 1, pp. 14-26, February 2018.

[3] P. Parthiban, B-C. Seet and X. J. Li, "Low-cost low-profile UHF RFID reader antenna with reconfigurable beams and polarizations," 2017 IEEE International Conference on RFID (RFID), Phoenix, 2017, pp. 81-87.

[4] J. Lim *et al*., "A balanced power amplifier utilizing the reflected input power," 2009 IEEE International Symposium on Radio-Frequency Integration Technology (RFIT), Singapore, 2009, pp. 88-91.

[5] Y. Zeng, Z. N. Chen, X. Qing and J. Jin, "A Directional, Closely Spaced Zero-Phase-Shift-Line Loop Array for UHF Near-Field RFID Reader Antennas," IEEE Transactions on Antennas and Propagation, vol. 66, no. 10, pp. 5639-5642, October 2018.

[6] C. Huang, C. Wang, J. Zhu and W. Tang, "A Reader Antenna for UHF Near-Field RFID Applications Based on the Segment-Line Oppositely Directed Currents," IEEE Antennas and Wireless Propagation Letters, vol. 17, no. 12, pp. 2159-2163, December 2018.

[7] J. Guo, H. Lan and Y. Yin, "A Near-Field UHF RFID Reader Antenna Without Dead Zones," 2018 International Conference on Microwave and Millimeter Wave Technology (ICMMT), Chengdu, China, 2018, pp. 1-3.

[8] J. Zhang and Z. Shen, "Dual-Band Shared-Aperture UHF/UWB RFID Reader Antenna of Circular Polarization," IEEE Transactions on Antennas and Propagation, vol. 66, no. 8, pp. 3886-3893, August 2018.

[9] X. Yi, L. Huitema and H. Wong, "Polarization and Pattern Reconfigurable Cuboid Quadrifilar Helical Antenna," IEEE Transactions on Antennas and Propagation, vol. 66, no. 6, pp. 2707-2715, June 2018.

[10] J. Li, H. Liu, S. Zhang, M. Luo, Y. Zhang and S. He, "A Wideband Single-Fed, Circularly-Polarized Patch Antenna With Enhanced Axial Ratio Bandwidth for UHF RFID Reader Applications," IEEE Access, vol. 6, pp. 55883-55892, October 2018.

[11] J. Zheng, Y. Yang, X. He, C. Mao, J. Gao and C. Zhou, "Multiple-port reader antenna with three modes for UHF RFID applications," Electronics Letters, vol. 54, no. 5, pp. 264-266, March 2018.

[12] D. Ding, J. Xia, L. Yang and X. Ding, "Multiobjective Optimization Design for Electrically Large Coverage: Fragment-Type Near-Field\/Far-Field UHF RFID Reader Antenna Design," IEEE Antennas and Propagation Magazine, vol. 60, no. 1, pp. 27-37, February 2018.

[13] J. Yan, C. Liu, X. Liu, J. Li, H. Guo and X. Yang, "A Switchable Near-/Far-Field Reader Antenna for UHF RFID Applications," IEEE Antennas and Wireless Propagation Letters, vol. 17, no. 5, pp. 789-793, May 2018.

[14] M. Lalkota, G. Gupta and A. R. Harish, "UHF reader antenna for near and far field RFID operation," 2018 IEEE International Conference on RFID (RFID), Orlando, FL, 2018, pp. 1-7.

[15] J. K. Pakkathillam, M. Kanagasabai and M. G. N. Alsath, "Compact Multiservice UHF RFID Reader Antenna for Near-Field and Far-Field Operations," IEEE Antennas and Wireless Propagation Letters, vol. 16, pp. 149-152, 2017.

[16] Y. Yao, C. Cui, J. Yu and X. Chen, "A Meander Line UHF RFID Reader Antenna for Near-field Applications," IEEE Transactions on Antennas and Propagation, vol. 65, no. 1, pp. 82-91, January 2017.

[17] W.S. Chen, K. L. Wong, and C.K. Wu "Inset microstripline-fed circularly polarized microstrip antennas", IEEE Transactions on Antenna and Propagation, vol. 48, no. 8, pp. 1253-1254, August 2000.

[18] Speedway r420 reader (2018, December 14). Impinj [Online]. Available: https://www.impinj.com/platform/connectivity/speedway-r420/

[19] Miniweb (2018, December 14). Smartrac-group [Online]. Available: https://www.smartrac-group.com/miniweb.html.

[20] Bling (2018, December 14). Smartrac-group [Online]. Available:: https://www.smartrac-group.com/bling.html